Available online at www.sciencedirect.com
SCIENCE DIRECT®
ELSEVIER
Journal of Computational and Applied Mathematics 168 (2004) 179–190
JOURNAL OF COMPUTATIONAL AND APPLIED MATHEMATICS
www.elsevier.com/locate/cam

Solution of radiative heat transfer problems with the discrete transfer method applied to triangular meshes

Véronique Feldheim*, Paul Lybaert[1]

Service de Thermique et Combustion, Faculté Polytechnique de Mons, Rue de l'Epargne 56, Mons B-7000, Belgium

Received 26 September 2002; received in revised form 13 May 2003

Abstract

The present communication deals with the solution of the radiative transfer equation in a gray absorbing media. The solution is performed on unstructured triangular meshes using the discrete transfer method (DTM). The application of the DTM to triangular meshes is detailed and discussed. The developed code is validated with benchmark cases and applied to pure radiative problem (with and without evaluation of the source term). The approach shows very good performances for the wall heat transfer evaluation. The discrete transfer method also presents a particular ray effect. This effect is clearly brought up with the study of radiative equilibrium between eccentric cylinders: wiggles can appear in the temperature field. To reduce this ray effect, the use of a great amount of rays is required to get a smooth (i.e. wiggle free) solution, in the case of pure radiative problems. The solution of coupled conductive–radiative problems or convective–radiative heat transfer necessitates less rays to obtain a converged solution.

MSC: 35K05; 80A20

Keywords: Radiative heat transfer; Discrete transfer method; Triangular meshes; Ray effect

1. Introduction

This paper presents the numerical solution of radiative heat transfer problems in rather complex shaped domains. The computation is performed in gray absorbing media and on unstructured triangular meshes. The context of the study is the application of a complete conductive–convective and radiative heat transfer code to the simulation of complex industrial problems, such as burners or

* Corresponding author.
E-mail address: veronique.feldheim@fpms.ac.be (V. Feldheim).
[1] Also for correspondence.

0377-0427/$ - see front matter
doi:10.1016/j.cam.2003.05.016

kilns. In many of these industrial processes, the temperature level is rather high and the radiative heat transfer plays a predominant role.

Among the numerous solution methods for the radiative transfer equation, we have chosen to work with the discrete transfer method (DTM). This method has been originally developed on structured cartesian meshes by Lockwood and Shah [3]. In the industrial application context, the discrete transfer method is advantageous because of its basic principle: the discretisation of the radiative intensity from the boundaries of the domain.

The radiative intensity varies with its location but also with the propagation direction. We then need a spatial discretisation scheme and also an angular discretisation. In the following sections we discuss the application of the discrete transfer method on unstructured triangular meshes.

We develop the distinctive features of the approach and validate it thanks to different benchmarks. The solution of the RTE along each ray is detailed, as well as the evaluation of the radiative source term and the distribution of the elementary source term between the nodes of each triangular element.

The results are compared with analytical solutions (for the simplest test cases), or with numerical results obtained by the zone method [1] and the finite volume method [5]. Two kinds of pure radiative transfer problems are considered i.e. with and without evaluation of the radiative source term. The influence of the space and angular discretisations are discussed.

2. The discrete transfer method on unstructured meshes

2.1. Governing equations

For a nonscattering gray medium, the radiative transfer equation (RTE) may be written, for a ray travelling along direction s, in the following form:

$$\frac{\mathrm{d}I}{\mathrm{d}s} = -\kappa I + \kappa I_{\mathrm{b}}(T), \tag{1}$$

where I is the radiant intensity in the s direction and $I = f(x, y, z, s, \tau)$, κ is the absorption coefficient and I_{b} the blackbody radiative intensity of the medium. The expression on the left-hand side of Eq. (1) represents the evolution of the intensity along the direction s inside a solid angle $\mathrm{d}\Omega$ around the propagation direction. The two terms on the right represent the changes in intensity due to absorption and emission, respectively.

If the walls of the domain are grey and perfectly diffuse surfaces, the boundary conditions are given by

$$I^{+} = \varepsilon I_{\mathrm{b}}(T) + \frac{1-\varepsilon}{\pi} \int_{\vec{s}\cdot\vec{n}<0} I^{-} |\vec{s}\cdot\vec{n}| \, \mathrm{d}\Omega,$$

where I^{+} is the radiant intensity leaving the surface, $I_{\mathrm{b}}(T)$ the blackbody intensity at the wall temperature, I^{-} the incident intensity on the surface and ε the wall emission factor.

Emission and absorption of radiation by the medium lead to a volumetric radiation source in the energy equation of the medium. It is given by

$$\dot{S}_r = \int_{4\pi} -\left(\frac{\mathrm{d}I}{\mathrm{d}s}\right) \mathrm{d}\Omega = \kappa \int_{4\pi} I \, \mathrm{d}\Omega - 4\pi\kappa I_{\mathrm{b}}(T) = \kappa \int_{4\pi} I \, \mathrm{d}\Omega - 4\kappa\sigma T^4.$$

The radiative heat flux is defined by: $\vec{q}_r(\vec{r}) = \int_{4\pi} I(\vec{r},\vec{s}) \cdot \vec{s}\, d\Omega$ and the source term is also given by: $\dot{S}_r = -\vec{\nabla}\vec{q}_r$.

2.2. Principles of the DTM

In the discrete transfer method [3], rays are fired in prescribed directions from discrete points located along the boundary. The evolution of the radiation intensity along each ray is then computed by solving the RTE. This evolution depends on the temperature variation along the ray, which is obtained from the temperatures at the nodes of the grid that is used to approximate the temperature field inside the computational domain.

The transposition of the DTM to unstructured meshes is based on the following approximations and choices (see Fig. 1):

- The temperature field is defined on an unstructured mesh of triangular elements, with the temperatures being stored at the nodes. The boundary of the domain is then approximated by a set of linear segments.
- The blackbody emissive power (i.e. T^4) is assumed to vary linearly in each triangular element. The assumption of an elementary value of T^4, equal to the average of the nodal values, does not lead to different results, for any spatial or angular discretisation.
- The radiation intensity is assumed to be uniform on every boundary segment, equal to the intensity value at the mid-point of the segment.
- The central point (P_i) of each segment on the boundary is considered [4] and the hemisphere centred on P_i is subdivided into a given number of solid angles with each solid angle defining a direction (ray).
- In two dimensional problems, each ray direction is defined by two angles, θ and ϕ, with θ being the angle between the normal to the boundary and the projection of the ray in the x–y plane, and ϕ being the angle between the ray and the x–y plane.

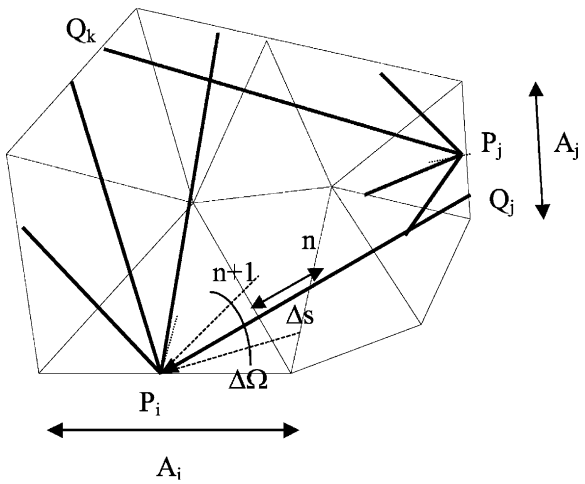

Fig. 1. Domain discretisation and ray definition.

- The points inside the domain where the radiative intensities have to be computed are the intersections of each ray with the triangular element sides.

2.3. Solution of the transfer equation along a ray

Starting from point P_i, each ray is traced until it hits another boundary. Let Q_j be the impingement point. Although, in general, Q_j is not the central point of a boundary segment, it is assumed that the radiation intensity at Q_j and at the central point P_j of the segment containing Q_j are equal (see Fig. 1).

Then starting from Q_j, the ray is traced back to the origin P_i and Eq. (1) has to be integrated analytically along the ray.

Inside each element, we have

$$\left(\frac{\partial T^4}{\partial s}\right)_e = \frac{T_{n+1}^4 - T_n^4}{s_{n+1} - s_n}$$

with

$$T_{n+1}^4 = aT_1^4 + (1-a)T_2^4, \tag{2}$$

$$T_n^4 = bT_1^4 + (1-b)T_3^4, \tag{3}$$

where n and $n+1$ are the intersections of the ray with the element sides; a and b define the relative positions of $n+1$ and n with respect to nodes $1,2$ and $1,3$ (see Fig. 2).

By integrating the RTE between n and $n+1$, we obtain the following recurrence relation:

$$I_{n+1} = I_n \mathrm{e}^{-\kappa\Delta s} + \frac{\sigma}{\pi} T_{n+1}^4 (1 - \mathrm{e}^{-\kappa\Delta s}) - \frac{\sigma}{\pi}\left(\frac{\partial T^4}{\partial s}\right)_e \frac{1}{\kappa}\left[1 - \mathrm{e}^{-\kappa\Delta s}(1+\kappa\Delta s)\right]. \tag{4}$$

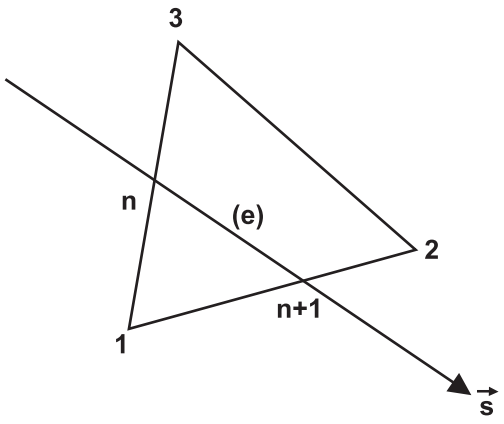

Fig. 2. Ray intersection with an element.

To initiate the solution of the recurrence equation, we need to know the intensities at the points Q_j. These are given from the boundary conditions. For a gray, perfectly diffuse wall, we have

$$I_{Q_j} \cong I_{P_j} = \frac{\dot{q}_{o,j}}{\pi} = \varepsilon_j \frac{\sigma T_j^4}{\pi} + (1-\varepsilon_j)\frac{\dot{q}_{i,j}}{\pi}$$

with the impinging flux $\dot{q}_{i,j}$ on the surface being given by

$$\dot{q}_{i,j} = \sum_{Q_k \text{ seen by } P_j} I_{Q_k P_j} |\vec{u}_{Q_k P_j}.\vec{n}_j| \Delta\Omega_{P_j Q_k} = \sum_{Q_k} I_{Q_k P_j} \cos\phi \cos\theta \Delta\Omega_{P_j Q_k}.$$

Unless the walls of the domain are black, the wall intensity depends on the intensity of all other rays: the calculations then follow an iterative procedure.

2.4. Evaluation of the radiative source term

Once all the intensities have been obtained, the radiative source term S in the energy equation can be easily evaluated. By referring to Fig. 1, a ray and its associated beam from P_i to Q_j penetrates a certain element. The contribution of this ray to the source term of the current element is given by

$$S^e_{P_i Q_j} = (I_n - I_{n+1})(\vec{n} \cdot \vec{u}_{P_i Q_j}) \Delta A_i \Delta\Omega_{P_i Q_j}.$$

The total source term for the element (e) is obtained by summing up all the contributions of all the rays crossing the current element

$$S^e_T = \sum_{P_i Q_j} S^e_{P_i Q_j}.$$

The contribution of a ray to the source term is proportional to $I_n - I_{n+1}$. Taking relations (2) and (3) into account, the recurrence relation (4) gives

$$I_n - I_{n+1} = f_n \left[I_n - \frac{\sigma}{\pi}(bT_1^4 + (1-b)T_3^4) \right] + f_{n+1} \left[I_n - \frac{\sigma}{\pi}(aT_1^4 + (1-a)T_2^4) \right]$$

with $f_{n+1} = 1 - (1/\kappa\Delta s)(1 - \mathrm{e}^{-\kappa\Delta s})$ and $f_n = (1/\kappa\Delta s)(1 - \mathrm{e}^{-\kappa\Delta s}) - \mathrm{e}^{-\kappa\Delta s}$.

To assign a portion of the source term to each node, we distribute it proportionally to the values of a, b, f_n and f_{n+1}. The following relations are used for the nodes 1, 2 and 3, respectively:

$$(f_n b + f_{n+1} a)\left(I_n - \frac{\sigma}{\pi} T_1^4 \right),$$

$$f_{n+1}(1-a)\left(I_n - \frac{\sigma}{\pi} T_2^4 \right),$$

$$f_n(1-b)\left(I_n - \frac{\sigma}{\pi} T_3^4 \right).$$

This source term distribution ensures physical temperature fields, particularly when studying problems of radiative equilibrium. In the last cases, the "a priori" simplest repartition (i.e. $\frac{1}{3}$–$\frac{1}{3}$–$\frac{1}{3}$) leads to

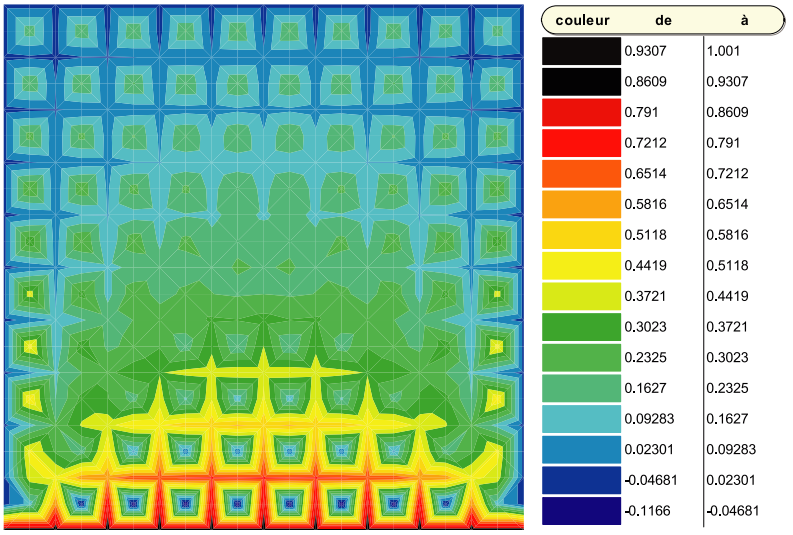

Fig. 3. σT^4 field in a square cavity in radiative equilibrium—source term distribution: $\frac{1}{3}$–$\frac{1}{3}$–$\frac{1}{3}$.

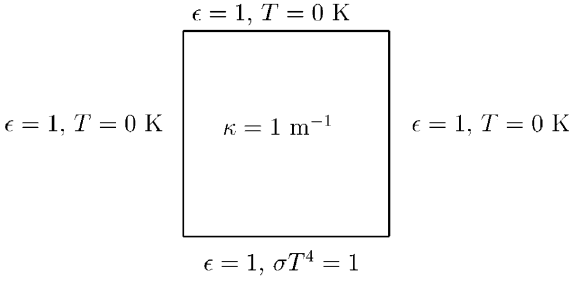

Fig. 4. Square cavity in radiative equilibrium—problem statement.

unphysical temperature field. This is shown in Fig. 3, that represents the temperature field in a square cavity in radiative equilibrium (description of the case in Fig. 4).

3. Applications to pure radiative problems

3.1. Pure radiative problems without source term evaluation

3.1.1. Gray absorbing medium in a quadrilateral cavity

This test case, already studied by Rousse [5], involves the irregular quadrilateral enclosure depicted in Fig. 5. The enclosure is assumed to be filled with an absorbing medium at constant temperature T_m, and the walls are assumed to be black and held at a temperature of 0 K. The (x, y) coordinates

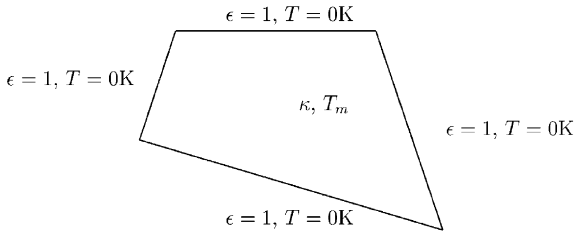

Fig. 5. Gray absorbing medium in a quadrilateral cavity—problem statement.

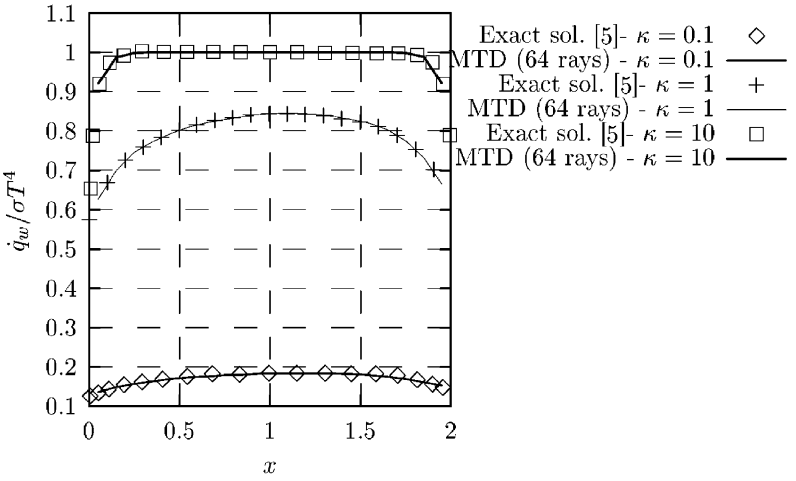

Fig. 6. Dimensionless radiant heat flux on the top surface for absorbing media bounded by a black quadrilateral enclosure—effect of the optical thickness.

of the four corners in the enclosure are: (0.00,0.90), (0.36,1.99), (2.36,1.99) and (3.03,0.00). Here, we study the effect of the optical thickness of the medium, τ, on the value of the dimensionless radiant heat flux at the top wall: $\dot{q}_w/\sigma T_m^4$. Our results were obtained with the same spatial and angular discretisation as for the CVFEM solution [5], executed on a 21×21 node mesh and with a (16×4) angular discretisation. The graph plotted in Fig. 6 shows the influence of the absorption coefficient on the radiative heat flux on the top surface; our results are compared with the exact solution given by Rousse. The mesh used in our computations is a regular grid of 21×21 nodes and constituted of triangular elements.

For thick media, the radiation from distant locations is mostly eliminated before it reaches a particular point: the radiative behaviour at any point depends only on its immediate surroundings. For the limit of a thin medium, $\tau = 0.1$, the surface radiant heat flux depends essentially on surface temperatures. As a result, the radiant heat flux at the top wall decreases with decreasing optical thickness because all surface temperatures are zero.

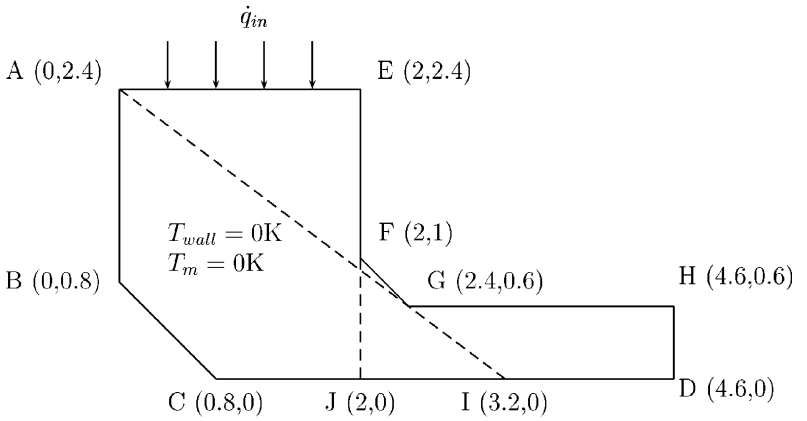

Fig. 7. Gray medium in a "L-shaped" cavity—problem statement.

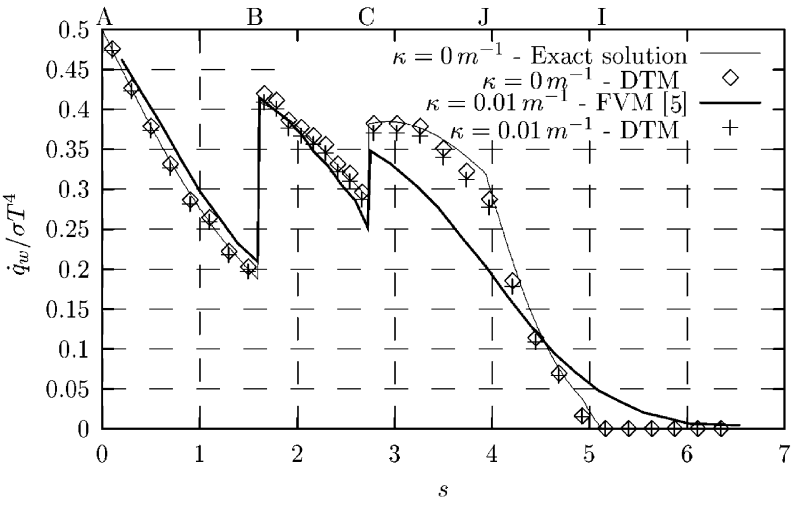

Fig. 8. Distribution of dimensionless radiant heat flux on the left-south wall A–D for $\kappa = 0$ m^{-1}—comparison with the zone method and for $\kappa = 0.01$ m^{-1}—comparison with the finite volume method—64 rays along θ for the DTM results.

3.1.2. Gray absorbing media in a "L-shaped" cavity

The second test case involves the "L-shaped" enclosure presented in Fig. 7. The enclosure is assumed to be filled with an emitting and absorbing medium at constant temperature $T_m = 0$ K, and the walls are assumed to be black and held at a constant zero temperature ($T_w = 0$ K) except for the top wall where $T = 100$ K. This is equivalent to assuming an outgoing radiant heat flux, $\dot{q}_{\text{in}}$ on the top wall between points A and E in Fig. 7.

Fig. 8 illustrates the dimensionless radiant heat flux at the left-south wall, identified by points A, B, C and D in Fig. 7. The surface radiant heat flux decreases with the distance away from point A,

because radiation is attenuated by absorption as it travels away from the top wall. The radiant heat flux impinging on a surface is also very sensitive to the orientation of this surface with respect to the source. The orientation of the wall changes at B and C, and this makes the left–south wall lie in a more direct line of sight from the source of radiation on the top wall (A–E). After the step (B–C), the radiant heat flux is seen to decrease to zero, as some points (beyond point I) do not "see" the radiation source on the top wall A–E, and because there is no reflexion and no emission from the boundaries.

The comparison of the DTM results and the zone method for the computation of the radiant heat flux with a transparent medium ($\kappa = 0\ \mathrm{m}^{-1}$) shows an excellent agreement between all the values. In particular, the zero value of the heat flux at point I is correctly predicted.

When considering a light emitting–absorbing medium ($\kappa = 0.01\ \mathrm{m}^{-1}$), our results are still very good: along the side ABCD, the radiant heat flux value is a little smaller than for a transparent medium. The comparison with the finite volume method (FVM) results shows that the latter method suffers from false (numerical) diffusion. The FVM cannot predict the zero value beyond point I, it underpredicts the radiant heat flux on point C and overpredicts the value along the side A–B. Moreover, in the FVM, the angular discretisation has to be adapted to the present geometry because of the orientation of the walls.

3.2. Problems of radiative equilibrium

3.2.1. Evaluation of the temperature field

In a problem of radiative equilibrium, the wall temperatures are imposed and the emitted radiation is equal to the absorbed one. The problem is to find the temperature field that set the source term equal to zero on each element in the domain, i.e. $\vec{\nabla}\vec{q}_r = 0$. This kind of problems allows to measure the ability of a method to correctly predict the source term in a radiative transfer problem.

Starting from a first approximation of the temperatures, the temperature field is updated using the following relationship:

$$\dot{S}_\mathrm{P} = S_\mathrm{P}^* + (T_\mathrm{P}^4 - T_\mathrm{P}^{*4}) \left(\frac{\partial \dot{S}_\mathrm{P}}{\partial T_\mathrm{P}^4} \right)^* = 0$$

(the values "*" are those from the previous iteration).

Or, put differently: $T_\mathrm{P}^4 = T_\mathrm{P}^{*4} + \alpha(S_\mathrm{P}/\Delta V)$ with $\alpha = (1/4\kappa\sigma)$.

3.2.2. Square cavity in radiative equilibrium

The problem of a square cavity in radiative equilibrium is detailed in Fig. 4. The comparison of our results with the exact solution [2] is shown in Fig. 9: we compare the evolution of the emissive power, σT^4, along the vertical centerline of the cavity. The graph in Fig. 9 shows the influence of the angular discretisation on the evolution of the emissive power. The results are obtained on a spatial mesh of 21×21 nodes (triangular elements) and for an optical thickness of $\tau = \kappa L = 1$ (L is the length of the cavity sides).

For a given spatial discretisation, the small wiggles around the exact solution vanish when increasing the angular discretisation (i.e. the number of rays along the θ direction). For a given number of rays, if the number of nodes increases, wiggles appear around the exact solution. This is a consequence of a ray effect and can be explained by the way the source term is computed: at the limit, if

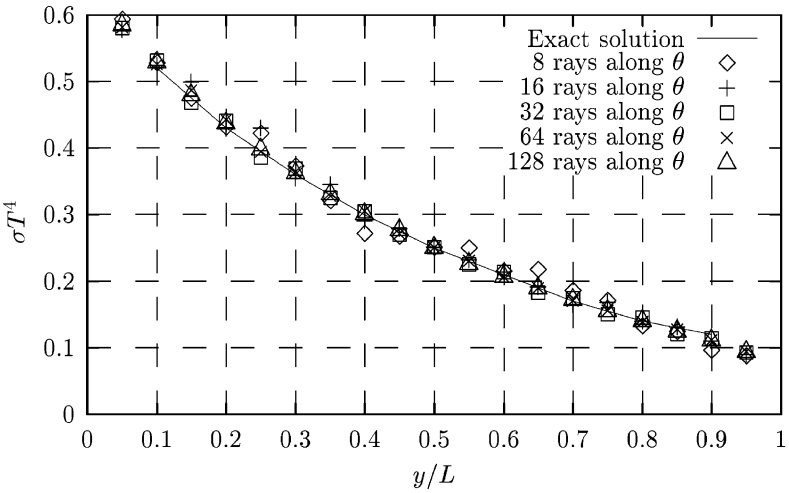

Fig. 9. Profile of σT^4 at $x/L = 0.5$ (21×21 nodes)—effect of angular discretisation ($\kappa L = 1$).

there are thousand elements and only two rays, some elements will not be passed through by these rays and the source term will not be accurate enough to give the right evolution of the emissive power.

3.2.3. Radiative equilibrium between two eccentric cylinders

The second case of radiative equilibrium concerns the study of the temperature field between two eccentric cylinders. Both cylinders have black walls, the inner cylinder has an unit emission power ($\sigma T_{\text{in}}^4 = 1$) and the outside cylinder is cold ($T_{\text{out}} = 0$ K). The diameter ratio is 2.6 and the relative eccentricity is $e_v/L = 0.652$ (e_v represents the distance between the centres of the two cylinders and $L = R_{\text{out}} - R_{\text{in}}$, the difference of the radius, is the reference length). The optical thickness is equal to one ($\tau = 1$). The mesh and the temperature field are represented in Fig. 10. On this figure, we also show the rays fired from each boundary side of the domain. The particular geometry of this case leads to ray concentration in some parts of the domain, having as bad consequence an unphysical temperature field, particularly below the small inner cylinder (when firing 8 rays from each boundary element). This ray effect can be attenuated by firing more rays along θ: the result of the angular sensitivity study is reported in Fig. 11. At least 64 rays along θ are required to get a smooth, decreasing evolution of the emissive power along the lower vertical centerline of this cavity.

4. Conclusions

We have presented in this paper the solution of the radiative heat transfer equation on triangular meshes with the discrete transfer method. The application of the original method on unstructured meshes has been detailed and the developed program validated with standard benchmark cases. Two kinds of problems have been addressed: pure radiative problems without source term evaluation and

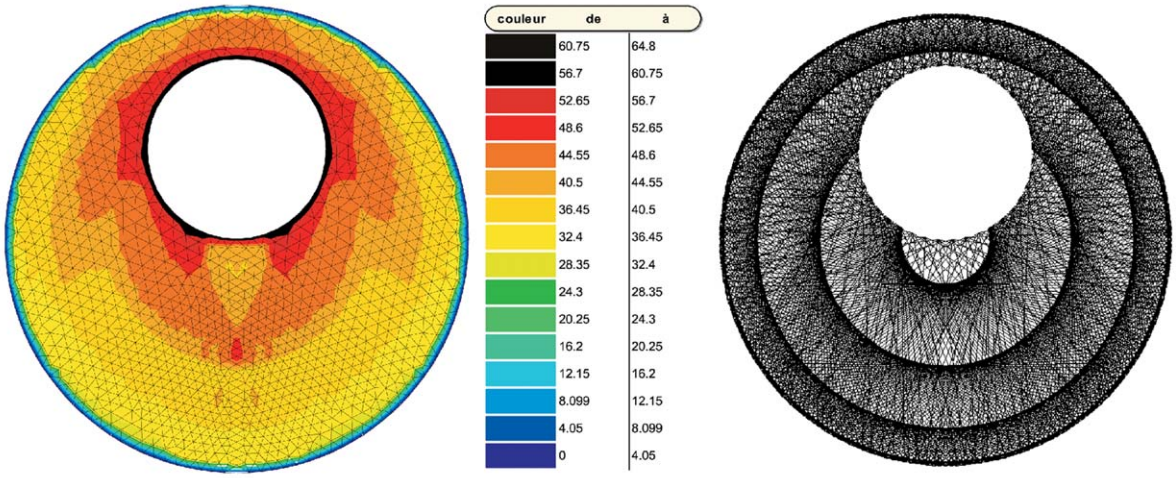

Fig. 10. Temperature field—representation of the rays (8 rays along θ)—$\tau = 1$.

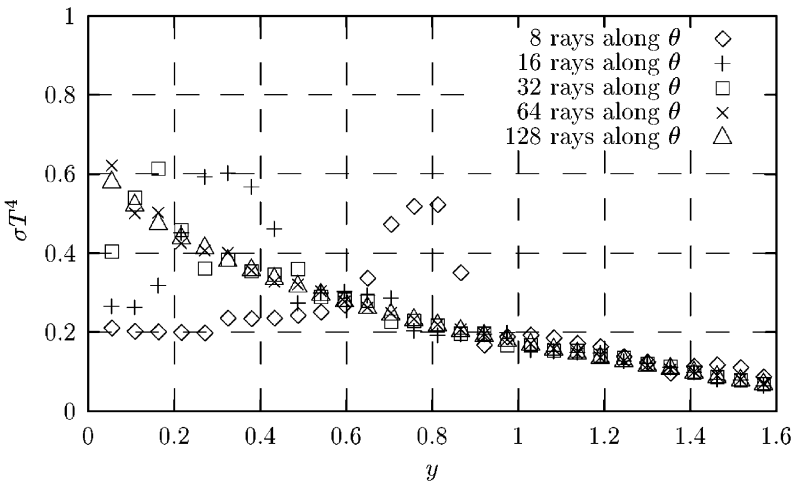

Fig. 11. Eccentric cylinders—evolution of σT^4 along the lower vertical centerline—influence of the angular discretisation—$\tau = 1$.

problems of radiative equilibrium. The results have been compared to those of classical methods: the zone method or the finite volume method.

The approach shows very good performances for the wall heat transfer evaluation. The discrete transfer method also presents a particular ray effect. This effect is clearly brought up with the study of radiative equilibrium between eccentric cylinders: wiggles can appear in the temperature field. To reduce this ray effect, the use of a great amount of rays is required to get a smooth (i.e. wiggle free) solution, in the case of pure radiative problems. The solution of coupled

conductive—radiative problems or convective—radiative heat transfer demands less rays to have a wiggle free solution, because of the smoothing of the solution by the conduction or convection mechanisms.

References

[1] S.H. Chan, Numerical methods for multidimensional radiative transfer analysis in participating media, Annual Review of Numerical Fluid Flow and Heat Transfer, Vol. 1, Chawla Edition, Hemisphere, Washington, DC, 1987 (Chapter 6).
[2] A.L. Crosbie, R.G. Schrenker, Radiative transfer in a two dimensional rectangular medium exposed to diffuse radiation, J. Quant. Spectrosc. Radiat. Transfer 31 (4) (1984) 339–371.
[3] F.C. Lockwood, N.G. Shah, A new radiation solution method for incorporation in general combustion prediction procedures, 18th International Symposium on Combustion, The Combustion Institute, Pittsburgh, PA, 1981, pp. 1405–1414.
[4] F.L. Meng, F. McKenty, R. Camarero, Radiative heat transfer by the discrete transfer method using an unstructured mesh, HTD Radiative Heat Transfer: Theory Applic., ASME 244 (1993) 55–66.
[5] D.R. Rousse, G. Gautier, J.F. Sacadura, Numerical predictions of two-dimensional conduction, convection and radiation heat transfer. II. Validation, Internat. J. Thermal Sci. 39 (2000) 332–353.